

Molecular tectonics: zinc coordination networks based on centric and acentric porphyrins bearing pyridyl units†

F. Sguerra, V. Bulach* and M. W. Hosseini*

Received 4th September 2012, Accepted 5th October 2012

DOI: 10.1039/c2dt32051g

Two new ligands, one symmetric **1** and the other acentric **2**, based on a porphyrin backbone bearing either two ethynylpyridyl or one pyridyl and one ethynylpyridyl coordinating groups connected to the porphyrin at two opposite *meso* positions have been designed and prepared. In the presence of a Zn(II) cation, they lead to the formation of neutral metallatectons **1**-Zn and **2**-Zn which self-assemble into coordination networks in the crystalline phase. Whereas the metallatecton **1**-Zn leads exclusively to the formation of grid type 2D networks, **2**-Zn generates two types of crystals with rod and rhombic morphologies. The rod type crystals are composed of a 1D zigzag type arrangement whereas crystals with rhombic morphology are composed of directional 2D grid type architecture. The packing of the latter leading to the formation of the crystal occurs in a centrosymmetric fashion causing thus the loss of directionality.

Introduction

Molecular tectonics¹ is a general approach dealing with molecular crystals for which some or all components called tectons^{2,3} are interconnected through specific interactions through molecular recognition⁴ or coordination events, into 1-, 2- or 3-D networks.⁵ Among various possible intermolecular interactions, the use of a coordination bond leading to coordination polymers⁶ or MOFs^{7–19} has attracted considerable attention over the last two decades.²⁰ This class of crystalline materials is a subgroup of molecular networks which are extended architectures presenting translational symmetry.²¹ The increasing interest in this type of hybrid assemblies arises from the endless possibilities that combinations of organic tectons and metallic centres or complexes offer. Furthermore, this class of periodic architectures displays useful properties such as storage,²² catalysis²³ and separation.²⁴ Although over the past few years many examples of coordination networks have been reported, the domain remains still challenging and of current interest.²⁵

Among the many organic coordinating tectons reported so far, the porphyrin based species are of particular interest.^{26–28} Indeed, in addition to its biological relevance, the porphyrin backbone offers photophysical and electrochemical properties resulting from its peculiar electronic structure. These may be of interest in materials sciences. Furthermore, its propensity to bind a vast variety of metal centres allows one to finely tune the above mentioned properties.

Here, we report on the design and synthesis of two new porphyrin based tectons and their use for the generation of 1- and 2-D networks in the presence of the Zn(II) cation.

Experimental part**Characterization techniques**

¹H-NMR and ¹³C-NMR spectra were recorded at room temperature on a Bruker (300 MHz) NMR spectrometer. UV-Vis absorption spectra were collected at room temperature on a UVIKON XL spectrometer from BIO-TEK instruments. Infrared spectra were measured on a Shimadzu FTIR-8400s equipped with a Pike Miracle ATR (Ge).

Mass spectra (ESI-MS) were recorded on a microTOF LC spectrometer (Bruker Daltonics, Bremen).

Single-crystal studies

Data were collected on a Bruker APEX8 CCD Diffractometer equipped with an Oxford Cryosystem liquid N₂ device at 173(2) K using a molybdenum microfocus sealed tube generator with mirror-monochromated Mo-K α radiation ($\lambda = 0.71073$ Å), operated at 50 kV/600 mA. The structures were solved using SHELXS-97 and refined by full matrix least-squares on F^2 using SHELXL-97 with anisotropic thermal parameters for all non-hydrogen atoms.²⁹ The hydrogen atoms were introduced at calculated positions and not refined (riding model).

Synthesis

General: All reagents were purchased from commercial sources and used without further purification. Compounds **4** and **9** are commercially available.

Laboratoire de Chimie de Coordination Organique, UMR CNRS 7140, Université de Strasbourg, Institut Le Bel, 4, rue Blaise Pascal, F-67000 Strasbourg, France. E-mail: hosseini@unistra.fr

† CCDC 899822–899825 (Crystallographic data for **1**-Zn-CH₂Cl₂, **1**-Zn, **2**-Zn-CHCl₃ and **2**-Zn in CIF format). For crystallographic data in CIF or other electronic format see DOI: 10.1039/c2dt32051g

Compounds **3**,³⁰ **5**–**7**³¹ and **8**³² were prepared according to reported procedures.

Compound 1. In a Schlenk tube, a solution of 5,15-dimesityl-10,20-dibromoporphyrin **6** (100 mg, 0.14 mmol, 1 equiv.), 4-ethynyl pyridine **8** (42 mg, 0.42 mmol, 3 equiv.), Pd₂dba₃ (64 mg, 0.07 mmol, 0.5 equiv.) and AsPh₃ (85.7 mg, 0.28 mmol, 2 equiv.) in degassed triethylamine (3 mL) and dry THF (7 mL) was heated at 75 °C for 1 h. The mixture was cooled to room temperature and the solvent was evaporated under reduced pressure. The product was washed with methanol (3 × 10 mL) and purified by column chromatography (Al₂O₃, CH₂Cl₂) to afford the pure compound as a green solid (84 mg, 80%).

¹H-NMR (300 MHz, CDCl₃) δ: −1.89 (s, br, 2H, NH), 1.87 (s, 12H, CH_{3ortho}), 2.66 (s, 6H, CH_{3para}), 7.32 (s, 4H, H_{meta}), 7.84 (d, *J* = 6.0 Hz, 4H, H_{pyridyl}), 8.72 (d, *J* = 4.8 Hz, 4H, H_{βpyr}), 8.82 (d, *J* = 6.0 Hz, 4H, H_{pyridyl}), 9.59 (d, *J* = 4.8 Hz, 4H, H_{βpyr}); ¹³C-NMR (90 MHz, CDCl₃) δ: 21.6 (CH₃), 30.9 (CH₃), 94.2 (C), 125.4 (CH), 128.0 (CH), 138.2 (CH), 139.1 (CH), 148.4 (C), 148.3 (C), 150.1 (CH). UV-Vis. (CH₂Cl₂) λ_{max}/nm (ε × 10⁴/L mol^{−1} cm^{−1}): 441 (34.17), 526 (0.91), 596 (3.39), 624 (1.85), 687 (2.09). IR (ATR)/cm^{−1} ν_{max}: 2205, 1734, 1591, 1558, 1538, 1524, 1491, 1471, 1452, 1399, 1368, 1344, 1315, 1261, 1213, 1194, 1159, 1001, 976, 947, 925, 858, 811, 796, 726, 704. *m/z* (HRM⁺): calc.: 749.339 [M + H⁺], found: 749.338.

Compound 2. In a Schlenk tube, a solution of 5,15-dimesityl-10-(pyridin-4-yl)-20-bromoporphyrin **11** (100 mg, 0.143 mmol, 1 equiv.), 4-ethynyl pyridine **8** (21.8 mg, 0.22 mmol, 1.5 equiv.), Pd₂dba₃ (32.7 mg, 0.036 mmol, 0.25 equiv.) and AsPh₃ (43.8 mg, 0.143 mmol, 1 equiv.) in degassed Et₃N (3 mL) and dry THF (7 mL) was heated at 75 °C for 2 h. The mixture was cooled to room temperature and the solvent was evaporated under reduced pressure. The product was washed with MeOH (3 × 10 mL) and purified by column chromatography (Al₂O₃, CH₂Cl₂) to afford the pure compound as a purple solid (70 mg, 68%).

¹H-NMR (300 MHz, CDCl₃) δ: −2.20 (s, br, 2H, NH), 1.88 (s, 12H, CH_{3ortho}), 2.67 (s, 6H, CH_{3para}), 7.33 (s, 4H, H_{meta}), 7.85 (br, 2H, H_{pyridyl}), 8.17 (br, 2H, H_{pyridyl}), 8.71 (s, 4H, H_{βpyr}), 8.78–8.88 (m, 4H, H_{pyridyl} and H_{βpyr}), 9.04 (s, br, H_{pyridyl}), 9.68 (d, *J* = 4.2 Hz, 2H, H_{βpyr}); ¹³C-NMR (90 MHz, CDCl₃) δ: 21.9 (CH₃), 22.1 (CH₃), 77.7 (C), 94.2 (C), 96.8 (C), 97.9 (C), 118.5 (C), 120.6 (CH), 125.8 (C), 128.4 (CH), 129.6 (CH), 132.4, 138.0 (CH), 138.6 (C), 139.7 (CH), 148.8 (CH), 150.4 (CH), 150.5 (C).

UV-Vis. (CH₂Cl₂) λ_{max}/nm (ε × 10⁴/L mol^{−1} cm^{−1}): 433 (44.71), 531 (1.26), 572 (2.66), 602 (0.74), 665 (1.17). IR (ATR)/cm^{−1} ν_{max}: 3326, 2964, 2919, 2539, 2323, 2200, 1591, 1561, 1536, 1472, 1536, 1472, 1454, 1404, 1377, 1345, 1218, 1193, 1151, 1070, 999, 977, 970, 929, 883, 850, 800, 789, 736, 728. *m/z* (HRM⁺): calc.: 725.339 [M + H⁺], found: 725.335.

Compound 10. 5,15-Dimesityl-10-bromoporphyrin **7** (147 mg, 0.235 mmol, 1 equiv.), 4-pyridine boronic acid **9** (60 mg, 0.5 mmol, 2.1 equiv.) and Na₂CO₃ (60 mg, 0.7 mmol, 3 equiv.) in a mixture of toluene (8 mL), MeOH (5 mL) and water (0.5 mL) were degassed with argon for 15 min. Then Pd(PPh₃)₄ (13.5 mg, 0.01 mmol, 0.05 equiv.) was added and the mixture was refluxed at 95 °C for 3 days. The solvent was evaporated under reduced pressure and the dark solid was purified by column

chromatography (Al₂O₃, CH₂Cl₂ to CH₂Cl₂–acetone 97 : 3). The compound was obtained as a purple solid (100 mg, 68%).

¹H-NMR (300 MHz, CDCl₃) δ: −2.82 (s, br, 2H, NH), 1.92 (s, 12H, CH_{3ortho}), 2.71 (s, 6H, CH_{3para}), 7.38 (s, 4H, H_{meta}), 8.25 (dd, *J* = 4.4 and 1.7 Hz, 4H, H_{pyridyl}), 8.86 (m, 4H, H_{βpyr}), 8.92 (d, *J* = 4.6 Hz, 2H, H_{βpyr}), 9.09 (dd, *J* = 4.4 and 1.7 Hz, 4H, H_{pyridyl}), 9.33 (d, *J* = 4.6 Hz, 2H, H_{βpyr}), 10.20 (s, 1H, H_{meso}); ¹³C-NMR (90 MHz, CDCl₃) δ: 21.5 (CH₃), 21.7 (CH₃), 104.9 (CH), 116.0 (C), 118.2 (C), 127.9 (C), 129.4 (CH), 130.3 (CH), 130.5 (CH), 130.9 (CH), 131.8 (CH), 137.8 (C), 138.0 (C), 139.4 (C), 148.2 (CH), 150.7 (C). UV-Vis. (CH₂Cl₂) λ_{max}/nm (ε × 10⁴/L mol^{−1} cm^{−1}): 419 (39.13), 508 (1.61), 539 (0.28), 582 (0.46), 637 (0.11). IR(ATR)/cm^{−1} ν_{max}: 1597, 1558, 1464, 1440, 1334, 1270, 1244, 1218, 1193, 1174, 1072, 1051, 997, 961, 844, 797, 784, 736, 705, 696. *m/z* (HRM⁺) calc.: 624.312 [M + H⁺], found: 624.311.

Compound 11. 5,15-Dimesityl-10-(pyridin-4-yl)porphyrin **10** (85 mg, 0.136 mmol, 1 equiv.) in CHCl₃ (65 mL) and pyridine (65 μL) was treated with NBS (27 mg, 1.1 equiv.) at 0 °C for 30 min. The mixture was quenched with acetone (15 mL). The solvent was evaporated under reduced pressure and the product was purified by column chromatography (Al₂O₃, CH₂Cl₂–acetone 95 : 5). The pure product was obtained as a purple solid (80 mg, 84%).

¹H-NMR (300 MHz, CDCl₃) δ: −2.58 (s, br, 2H, NH), 1.85 (s, 12H, CH_{3ortho}), 2.66 (s, 6H, CH_{3para}), 7.32 (s, 4H, H_{meta}), 8.18 (dd, *J* = 4.4 and 1.5 Hz, 2H, H_{pyridyl}), 8.72 (s, 4H, H_{βpyr}), 8.78 (d, *J* = 4.8 Hz, 2H, H_{βpyr}), 9.04 (dd, *J* = 4.4 and 1.5 Hz, 2H, H_{pyridyl}), 9.64 (d, *J* = 4.8 Hz, 2H, H_{βpyr}); ¹³C-NMR (90 MHz, CDCl₃) δ: 21.5 (CH₃), 21.6 (CH₃), 103.0 (CBr), 116.4 (C), 119.5 (C), 127.9 (CH), 129.3 (CH), 137.8 (C), 138.1 (CH), 139.3 (C), 148.3 (CH), 150.0 (C). UV-Vis. (CH₂Cl₂) λ_{max}/nm (ε × 10⁴/L mol^{−1} cm^{−1}): 419 (42.60), 517 (1.70), 551 (0.72), 595 (0.49), 651 (0.41). IR(ATR)/cm^{−1} ν_{max}: 3342, 3075, 2919, 2360, 2343, 1594, 1578, 1472, 1400, 1348, 1213, 1188, 1068, 971, 881, 846, 815, 801, 788, 737, 723, 657, 642. *m/z* (HRM⁺) calc.: 702.223 [M + H⁺], found: 702.223.

Crystallisation conditions

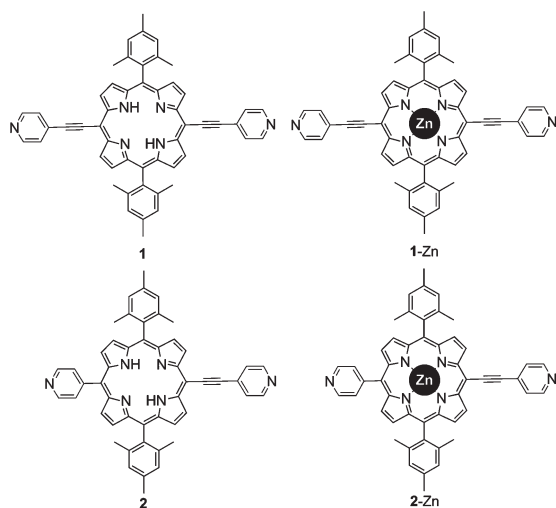
1-Zn: in a crystallization tube (4 mm diameter, 15 cm height), upon slow diffusion at room temperature of a MeOH solution (2 mL) of Zn(OAc)₂ (2 mg, 4 mmol L^{−1}) into a CH₂Cl₂ solution (0.5 mL) of compound **1** (0.38 mg, 1 mmol L^{−1}) purple crystals of **1-Zn** were obtained after 14 days.

2-Zn: in a crystallization tube (4 mm diameter, 15 cm height), upon slow diffusion at room temperature of a MeOH solution (2 mL) of Zn(OAc)₂ (2 mg, 4 mmol L^{−1}) into a CHCl₃ solution (0.5 mL) of compound **2** (0.36 mg, 1 mmol L^{−1}) two types of purple crystals (rod and rhombic morphologies representing ca. 90% and 10% respectively) were obtained after 10 days.

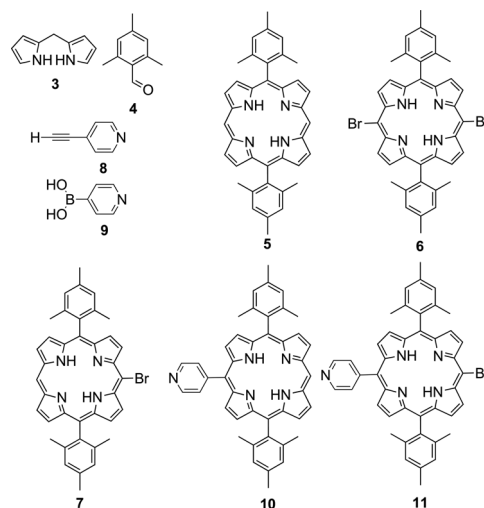
Results and discussion

Design of ligands **1** and **2**

The majority of the reported coordination networks is often based on two or three component systems. Furthermore, since



Scheme 1



Scheme 2

usually coordination networks are obtained upon combining metal cations and organic tectons, if the charge neutrality is not ensured by the organic tecton, the crystal contains anions as counter ions. In order to reduce the number of components and to avoid the presence of anions, one may use a self-complementary neutral metallatecton comprising a metal centre and an organic moiety bearing peripheral coordinating sites. It has been shown that this may be achieved by using metalporphyrin derivatives.^{33–40} Along this idea, compounds **1** and **2** (Scheme 1) were designed. These compounds are ligands offering three coordinating poles,⁴¹ *i.e.* the tetraaza core of a porphyrin and two peripheral monodentate pyridyl units. The binding of metal centres such as the Zn(II) cation, adopting the penta- or hexa-coordination mode, by **1** and **2** leads to the formation of **1-Zn** and **2-Zn** neutral complexes which, owing to the presence of two divergently oriented peripheral pyridyl units and the coordination extension possibility offered by the metal centre located within the core of the porphyrin, must behave as self-complementary metallatectons, leading thus to the formation of infinite neutral coordination networks.

Compounds **1** and **2** are symmetric and unsymmetrical porphyrin based ligands bearing two peripheral pyridyl units at the *meso* positions 10 and 20. The remaining two *meso* positions are occupied by two mesityl groups for solubilisation purposes. For compound **1**, an ethynyl spacer is used to connect the pyridyl group to the porphyrin backbone. Examples of porphyrin derivatives bearing ethynylpyridyl units have been reported.^{42,43} For compound **2** whereas one of the two pyridyl units is directly connected, for the other one, an ethynyl spacer is used. In principle, owing to the centric nature of the self-complementary metallatecton **1-Zn**, one would expect the formation of centrosymmetric architectures, whereas for the acentric tecton **2-Zn**, directional architectures may be expected.^{44–46}

Synthesis of ligands **1** and **2**

The synthetic strategy adopted for the preparation of ligands **1** and **2** is based on the common 5,15-dimesitylporphyrin precursor **5** (Scheme 2). The latter was synthesised following a

reported procedure by Lindsey *et al.*³¹ upon condensation of the dipyrin **3**³⁰ with the mesitylaldehyde **4**.

The porphyrin **5** may be selectively mono- or dibrominated at the unsubstituted *meso* positions 10 and 20 using 1 or 2 equiv. of NBS respectively.³¹

For the synthesis of compound **1**, a Sonogashira coupling reaction between the dibromo derivative **6** and 4-ethynylpyridine **8** was used. Two types of conditions have been tested for this coupling reaction. The first one was based on the use of Pd(PPh₃)Cl₂ and copper iodide as catalysts.⁴⁷ Although under these conditions compounds **1** could be obtained in 90% yield, unfortunately the ligand was contaminated with 8% of the **1-Cu** complex and the separation was found to be rather difficult and tedious. In order to avoid the metallation of the porphyrin backbone, another route based on a mixture of Pd₂(dba)₃ and AsPh₃ as the catalyst was explored.⁴⁸ Under this copper free condition, compound **1** could be obtained although with lower yields (60–80%).

For the synthesis of **2**, the monopyridyl derivative **10** was first prepared using a Suzuki coupling reaction between monobromoporphyrin **7** and 4-pyridineboronic acid **9** in the presence of Pd(PPh₃)₄ and sodium carbonate.⁴⁹ The reaction under reflux in toluene or in DMF at 120 °C failed and led to the dehalogenation of porphyrin **7**. However, in a biphasic medium (toluene/methanol/water),⁵⁰ the desired compound **10** was obtained in 68% yield. The latter was transformed into its brominated derivative **11** in 84% yield upon treatment with NBS in CHCl₃ at 0 °C. Finally, using the copper free conditions mentioned above for the synthesis of **1**, compound **2** was obtained in 68% yield upon a Sonogashira coupling between bromo derivative **11** and 4-ethynylpyridine **8**.

Structural investigations of coordination networks formed by **1-Zn** and **2-Zn**

The generation of coordination networks was achieved by self-assembly processes by reacting ligand **1** or **2** with zinc acetate. At room temperature, upon slow diffusion of a MeOH solution of Zn(OAc)₂ into a CH₂Cl₂ or CHCl₃ solution of porphyrin **1** or

2, suitable crystals were obtained. Under the crystallisation process, ligands **1** and **2** were metallated affording thus the metallatectons **1-Zn** and **2-Zn** respectively (Scheme 1). The crystalline materials thus obtained (see the experimental section) were structurally studied using X-ray diffraction methods on single crystals (Table 1).

For **1-Zn**, the structural investigation revealed that the crystal (monoclinic, $P2(1)/n$) is composed of **1-Zn** and CH_2Cl_2 solvent molecules which were found to be disordered over two positions. For the solvent molecules, occupying the empty space, no specific interactions with the tecton are observed.

The porphyrin backbone is quasi-planar. The two N atoms of the two ethynylpyridine units are located above and below the mean plane of the porphyrin by 1.18 Å (Fig. 1). The two mesityl units and pyridyl groups are tilted with respect to the porphyrin plane by 80.2° and 35.7° respectively.

The Zn(II) cation, located in the centre of the porphyrin backbone, is hexacoordinated with a deformed octahedral coordination geometry. Its coordination sphere is composed of 6 N atoms, among which four belong to the porphyrin tetraaza core with a Zn–N distance of *ca.* 2.06 Å and the remaining two apical positions are occupied by two N atoms of two pyridyl units belonging to two consecutive metallatectons **1-Zn** with a Zn–N distance of 2.380 (5) Å. The two pyridyl groups are not perpendicular to the porphyrin mean plane but tilted with an angle of 63.7°. Owing to the hexacoordination of the Zn cation, the overall architecture is a 2D coordination network of the grid type (Fig. 2). The distance between two consecutive Zn(II) cations within the grid is 12.51 Å. The dihedral angle between consecutive porphyrin units is 77.6°.

Consecutive sheets are packed in a parallel fashion. They are not eclipsed but staggered (space group $P2_1/n$). The distance between consecutive sheets is 8.02 Å. The shortest distance between Zn atoms belonging to two consecutive 2D grids is 8.02 Å. The packing mode leads to the formation of channels

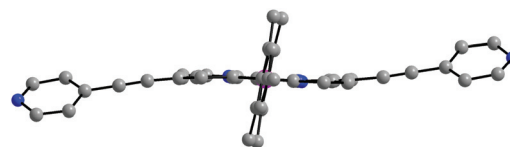


Fig. 1 A portion of the structure of the 2D grid-type architecture generated by the self-complementary metallatecton **1-Zn** showing the orientation of the mesityl and pyridyl groups and the location of the N atom of the two pyridyl units above and below the mean plane of the porphyrin. H atoms are not represented for clarity. For distances and angles see text.

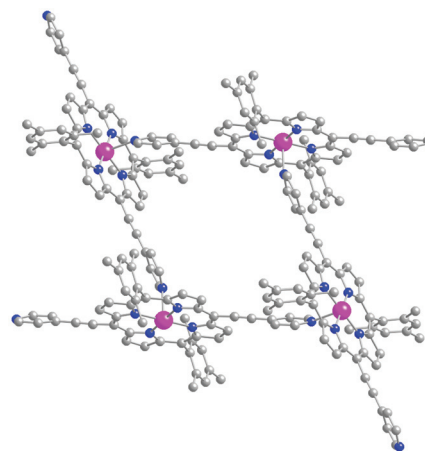


Fig. 2 A portion of the 2D coordination network generated by **1-Zn** showing the connectivity pattern between consecutive units. The grid type architecture is generated owing to the hexacoordination of the Zn cation allowing thus the interconnection of consecutive units. H atoms and CH_2Cl_2 solvent molecules are not represented for clarity. For bond distances and angles see text.

Table 1 Crystallographic parameters recorded at 173 K for **1-Zn** and **2-Zn**

	1-Zn · CH_2Cl_2	1-Zn	2-Zn · CHCl_3	2-Zn
Empirical formula	$\text{C}_{53}\text{H}_{40}\text{Cl}_2\text{N}_6\text{Zn}$	$\text{C}_{52}\text{H}_{38}\text{N}_6\text{Zn}$	$\text{C}_{51}\text{H}_{39}\text{Cl}_3\text{N}_6\text{Zn}$	$\text{C}_{50}\text{H}_{38}\text{N}_6\text{Zn}$
Molecular weight	897.18	812.25	907.60	788.23
Crystal system	Monoclinic	Monoclinic	Orthorhombic	Orthorhombic
Space group	$P2(1)/n$	$P2(1)/n$	$Pccn$	$Pccn$
<i>a</i> (Å)	11.3103(9)	10.7971(19)	19.7276(4)	16.1357(7)
<i>b</i> (Å)	13.8466(12)	14.170(3)	30.6924(6)	32.4593(14)
<i>c</i> (Å)	15.1616(12)	14.493(2)	14.4077(3)	15.6512(7)
α (°)	90	90	90	90
β (°)	102.876(4)	109.694(4)	90	90
γ (°)	90	90	90	90
<i>V</i> (Å ³)	2314.7(3)	2087.7(6)	8723.7(3)	8197.4(6)
<i>Z</i>	2	2	8	8
Colour	Purple	Purple	Purple	Purple
Crystal dim (mm ³)	0.14 × 0.12 × 0.07	0.14 × 0.12 × 0.07	0.12 × 0.08 × 0.04	0.12 × 0.12 × 0.08
<i>D</i> _{calc} (g cm ⁻³)	1.287	1.292	1.382	1.277
<i>F</i> (000)	928	844	3744	3280
μ (mm ⁻¹)	0.688	0.632	0.791	0.642
Wavelength (Å)	0.71073	0.71073	0.71073	0.71073
Number of data meas.	25 988	18 727	124 534	21 642
Number of data with $I > 2\sigma(I)$	6496 [<i>R</i> (int) = 0.0921]	4637 [<i>R</i> (int) = 0.0550]	9810 [<i>R</i> (int) = 0.0402]	9049 [<i>R</i> (int) = 0.0703]
<i>R</i>	<i>R</i> ₁ = 0.1061, <i>wR</i> ₂ = 0.2744	<i>R</i> ₁ = 0.0503, <i>wR</i> ₂ = 0.0844	<i>R</i> ₁ = 0.0674, <i>wR</i> ₂ = 0.1809	<i>R</i> ₁ = 0.0782, <i>wR</i> ₂ = 0.2045
<i>R</i> _w	<i>R</i> ₁ = 0.1676, <i>wR</i> ₂ = 0.3070	<i>R</i> ₁ = 0.0970, <i>wR</i> ₂ = 0.0886	<i>R</i> ₁ = 0.0864, <i>wR</i> ₂ = 0.1978	<i>R</i> ₁ = 0.1488, <i>wR</i> ₂ = 0.2434
GOF	1.106	1.000	1.029	1.031

filled with CH_2Cl_2 solvent molecules. Furthermore, the available space is occupied by the mesityl groups belonging to consecutive layers (Fig. 3).

The desolvation of crystals of **1**-Zn was studied on the same crystal. The removal of the CH_2Cl_2 molecules was achieved at room temperature over a period of 24 h. An X-ray diffraction study revealed a single-crystal-to-single-crystal transformation. While both the space group (monoclinic, $P2(1)/n$) and the connectivity pattern (grid type architecture) are conserved upon removal of the solvent, the metrics however undergoes significant changes. The Zn(II) cation remains hexacoordinated with a deformed octahedral coordination geometry (Fig. 4).

For the organic tecton, the dihedral angle of 24.3° between the porphyrin mean plane (24 atoms) and the ethynylpyridine moieties is considerably smaller than the one observed for the solvated crystal (35.7°). However, the orientation of the two mesityl groups remains almost unchanged.

The deviation from planarity of tecton **1** is enhanced. Indeed, the distance (1.84 Å) between the N atoms of the pyridyl units and the mean plane of the porphyrin backbone is considerably larger than the one observed for the solvate (1.18 Å) (Fig. 5).

The tilt angle between the ethynylpyridine units and the porphyrin mean plane is slightly enhanced from 63.7° for the

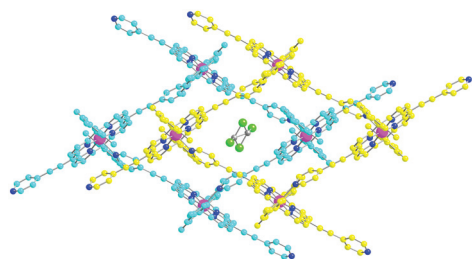


Fig. 3 A portion of the structure of the 2D coordination network generated by **1**-Zn showing the packing of consecutive sheets as well as the localisation of the CH_2Cl_2 solvent molecules in the channels. H atoms are not represented for clarity. The carbon atoms of consecutive sheets are differentiated by colour for clarity. For distances and angles see text.

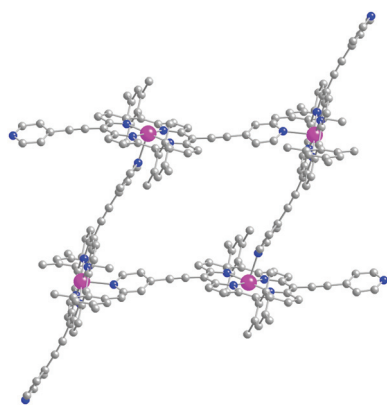


Fig. 4 A portion of the structure of the desolvated crystals of **1**-Zn showing the deformation of the grid type architecture upon removal of CH_2Cl_2 solvent molecules. H atoms are not represented for clarity. For bond distances and angles see text.

solvate to 69.3° . Finally, the removal of the solvent molecules leads to the shrinking of the consecutive sheets by *ca.* 1 Å. Consequently, the volume of 2087 \AA^3 observed for the desolvated crystal represents a *ca.* 10% decrease when compared to the solvated crystal (2314 \AA^3).

The reversibility of the solvation/desolvation process was also studied. Unfortunately, upon diffusion of CH_2Cl_2 vapours into desolvated crystals, an amorphous powder was obtained.

The unsymmetrical ligand **2** in the presence of the zinc(II) cation leads to the metallatecton **2**-Zn (Scheme 1). As for compound **1**, the metallation process takes place during the crystallisation process. However, whereas in the case of **1** only one type of crystal is formed, for **2**, two types of crystals with distinct morphologies are obtained (Fig. 6).

The rod type crystals (Fig. 6 left) dominate and represent the major component of the mixture (*ca.* 80–90%) whereas the rhombic crystals (Fig. 6 right) are the minor component.

X-ray diffraction analysis on crystals with rod type morphology revealed the formation of a 1D zigzag type architecture (Table 1) (Fig. 7). The crystal, in addition to the **2**-Zn entity, contains a CHCl_3 solvent molecule. In marked contrast with the 2D network formed by **1**-Zn and resulting from the hexacoordination of metal centres, for the 1D network, the zinc cation is penta-coordinated. The coordination geometry of the cation is square based pyramidal and its coordination sphere is composed of four N atoms belonging to the porphyrin backbone occupying the square base with an average Zn–N distance of *ca.* 2.06 Å. The apical position is occupied by the N atom ($d_{\text{Zn-N}} = 2.177(3) \text{ \AA}$) of a pyridyl unit belonging to the consecutive **2**-Zn complex indicating that only one out of the two pyridyl units of **2** is engaged in the connectivity pattern. It is worth noting that among the two types of pyridyl groups, only the one directly connected to the *meso* position of the porphyrin is bound to the metal centre whereas the pyridyl of the ethynylpyridine moiety remains unbound. However, the latter interacts with consecutive 1D networks by π - π interactions.

The porphyrin backbone is slightly domed and the Zn cation is located above the porphyrin mean plane with a distance of

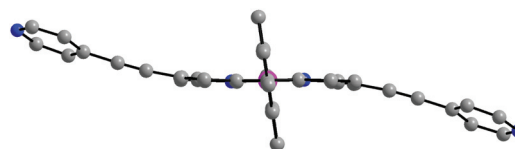


Fig. 5 A portion of the structure of the desolvated crystal of **1**-Zn showing the orientation of the mesityl and pyridyl groups. H atoms are not represented for clarity. For distances and angles see text.

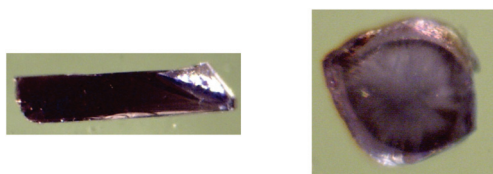


Fig. 6 Photographs of the two types of crystals with rod (left) and rhombic morphologies obtained upon combining compound **2** with the Zn cation.

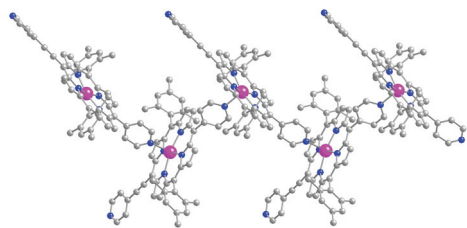


Fig. 7 A portion of the structure of **2-Zn** showing the formation of a 1D zigzag type arrangement. Among the two peripheral pyridyl units, only the one directly connected to the porphyrin backbone is engaged in the connectivity pattern. H atoms and CHCl_3 solvent molecules are not represented for clarity. For bond distances and angles see text.

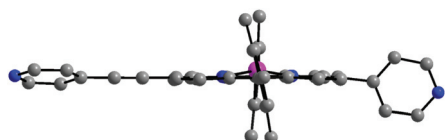


Fig. 8 A portion of the crystal structure of **2-Zn** showing the orientation of the mesityl and pyridyl groups. H atoms and CHCl_3 solvent molecules are not represented for clarity. For distances and angles see text.

0.31 Å. The dihedral angles between the mesityl and ethynylpyridyl units and the porphyrin mean plane are *ca.* 80° and 14° respectively (Fig. 8).

Whereas the N atom of the ethynylpyridine unit is slightly above the mean plane of the porphyrin backbone with a distance of 0.14 Å, the N atom of the pyridine moiety directly connected to the porphyrin is located below with a distance of 0.48 Å (Fig. 8). The dihedral angle between the porphyrin and the pyridyl group bound to the Zn cation is 76.4° which is slightly higher than the one observed for the grid type structures discussed above.

The X-ray diffraction study on crystals with rhombic morphology revealed the formation of a directional grid type architecture (Fig. 9). The crystal (orthorhombic, *Pccn*, Table 1) is only composed of **2-Zn** complexes.

The Zn cation, as in the case of **1-Zn**, is hexacoordinated with a distorted octahedral coordination geometry. The square base of the latter is occupied by four N atoms of the porphyrin core with an average Zn–N distance of *ca.* 2.05 Å. The two apical positions are occupied by two N atoms belonging to a pyridyl and an ethynylpyridyl unit belonging to consecutive tectons **2-Zn** with again an average Zn–N distance of *ca.* 2.35 Å.

The macrocyclic part of tecton **2** is slightly deformed. However, the deformation is more pronounced than the one observed for the 1-D network discussed above. In contrast with all three structures mentioned above, *i.e.* the 2D grid type architectures obtained with **1-Zn** (both the solvated and desolvated crystals) and the 1D network observed for **2-Zn**, the N atoms of both the pyridyl and ethynylpyridyl units are located above the mean plane of the porphyrin with distances of 0.74 Å and 1.27 Å respectively (Fig. 10). The pyridyl and ethynylpyridyl units are tilted with respect to the porphyrin backbone by 65.7° and 19.5° respectively. The distance between two adjacent Zn cations within the grid type structure is 10.06 Å.

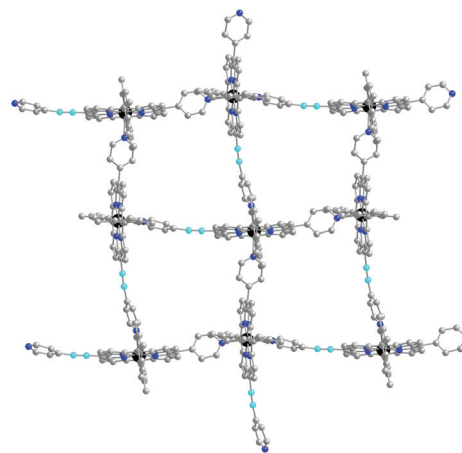


Fig. 9 A portion of the 2D coordination network generated by **2-Zn** (crystals with rhombic morphology) showing the connectivity pattern between consecutive units. The grid type architecture is directional. The C atoms of the ethynyl units are differentiated by colour (blue) and H atoms are not represented for clarity. For bond distances and angles see text.

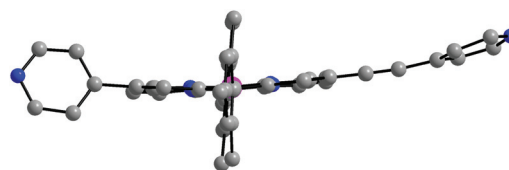


Fig. 10 A portion of the crystal structure of **2-Zn** (rhombic morphology) showing the orientation of the mesityl and pyridyl groups. H atoms are not represented for clarity. For distances and angles see text.

It is worth noting that, owing to the presence of one pyridyl and one ethynylpyridyl unit located at the axial positions of the metal centre, the grid type layer is directional, *i.e.* within a single grid, the connectivity sequence is of the type (Py, Py, ethynylpyridyl, ethynylpyridyl).

Consecutive grids are packed in a parallel fashion in the AABB mode. They are not eclipsed but staggered (space group *Pccn*). The distance between consecutive sheets is 8.22 Å. This mode of packing leads to the occupation of empty spaces by mesityl groups belonging to consecutive 2D networks (Fig. 11).

Although the grid type structure is directional, owing to the centrosymmetric packing of consecutive grids following the AABB mode, the overall crystal is not directional (Fig. 11).

Conclusions

In conclusion, the two centric and acentric ligands **1** and **2** based on a porphyrin backbone bearing two peripheral pyridyl coordinating groups at two opposite *meso* positions lead in the presence of a Zn(II) cation to the formation of two metallatectons **1-Zn** and **2-Zn**. The latter being self complementary building blocks self-assemble into coordination networks. Whereas in the case of **1**, a 2D grid type architecture is formed, for **2**, two types of crystals with rod or square type morphology are obtained. Interestingly, the square type crystals are formed upon packing

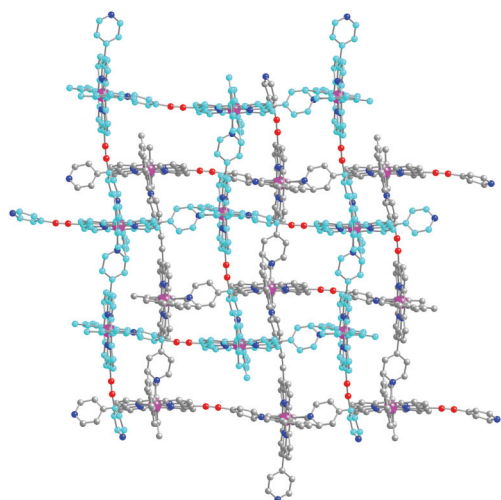


Fig. 11 A portion of the 2D coordination network generated by 2-Zn (crystals with rhombic morphology) showing the packing of two consecutive sheets. Owing to the antiparallel packing of consecutive sheets in an AABB mode, the overall architecture is centric. The C atoms of consecutive sheets are differentiated by colour (blue and grey) and H atoms are not represented for clarity. For distances see text.

of directional 2D grid type networks. Owing to the centrosymmetric arrangement of the directional sheets, the directionality is lost. We are currently investigating the possibility of avoiding the centric packing by the introduction of chirality in the porphyrin backbone.

We thank the University of Strasbourg, the Institut Universitaire de France (IUF), the International Centre for Frontier Research in Chemistry (icFRC), the C.N.R.S. and the Ministry of Research (Ph.D. fellowship to F. S.) for financial support.

Notes and references

- 1 S. Mann, *Nature*, 1993, **365**, 499.
- 2 (a) M. Simard, D. Su and J. D. Wuest, *J. Am. Chem. Soc.*, 1991, **113**, 4696; (b) J. D. Wuest, *Chem. Commun.*, 2005, 5830.
- 3 M. W. Hosseini, *Acc. Chem. Res.*, 2005, **38**, 313.
- 4 J.-M. Lehn, *Supramolecular Chemistry: Concepts and Perspectives*, VCH, Weinheim, 1995, p. 1494.
- 5 M. W. Hosseini, *CrystEngComm*, 2004, **6**, 318.
- 6 (a) B. F. Abrahams, B. F. Hoskins and R. Robson, *J. Am. Chem. Soc.*, 1991, **113**, 3606; (b) S. R. Batten and R. Robson, *Angew. Chem., Int. Ed.*, 1998, **37**, 1460.
- 7 C. Kaes and M. W. Hosseini, NATO ASI Series, C518, ed. J. Viciana, 1998, 53–66.
- 8 A. J. Blake, N. R. Champness, P. Hubberstey, W.-S. Li, M. A. Withersby and M. Schröder, *Coord. Chem. Rev.*, 1999, **193**, 117.
- 9 B. Moulton and M. J. Zaworotko, *Chem. Rev.*, 2001, **101**, 1629.
- 10 M. Eddaoudi, D. B. Moler, H. Li, B. Chen, T. M. Reineke, M. O’Keeffe and O. M. Yaghi, *Acc. Chem. Res.*, 2001, **34**, 319.
- 11 (a) C. Janiak, *Dalton Trans.*, 2003, 2781; (b) C. Janiak and J. L. Vieth, *New J. Chem.*, 2010, **34**, 2366.
- 12 L. Carlucci, G. Ciani and D. M. Proserpio, *Coord. Chem. Rev.*, 2003, **246**, 247.
- 13 (a) S. Kitagawa, R. Kitaura and S. Noro, *Angew. Chem., Int. Ed.*, 2004, **43**, 2334; (b) S. Kitagawa and K. Uemura, *Chem. Soc. Rev.*, 2005, **34**, 109.
- 14 G. Férey, C. Mellot-Draznieks, C. Serre and F. Millange, *Acc. Chem. Res.*, 2005, **38**, 218.
- 15 D. Bradshaw, J. B. Claridge, E. J. Cussen, T. J. Prior and M. J. Rosseinsky, *Acc. Chem. Res.*, 2005, **38**, 273.
- 16 D. Maspoch, D. Ruiz-Molina and J. Veciana, *Chem. Soc. Rev.*, 2007, **36**, 770.
- 17 J. R. Long and O. M. Yaghi, *Chem. Soc. Rev.*, 2009, **38**, 1213.
- 18 W. L. Leong and J. J. Vittal, *Chem. Rev.*, 2011, **111**, 688.
- 19 M. Yoon, R. Srirambalaji and K. Kim, *Chem. Rev.*, 2012, **112**, 1196.
- 20 Special issue on Metal–Organic Frameworks in *Chem. Rev.*, vol. 2, 2012.
- 21 M. W. Hosseini, *Chem. Commun.*, 2005, 5825.
- 22 (a) M. P. Suh, H. J. Park, T. K. Prasad and D.-W. Lim, *Chem. Rev.*, 2011, **112**, 782; (b) K. Sumida, D. L. Rogow, J. A. Mason, T. M. McDonald, E. D. Bloch, Z. R. Herm, T.-H. Bae and J. R. Long, *Chem. Rev.*, 2011, **112**, 724.
- 23 M. Yoon, R. Srirambalaji and K. Kim, *Chem. Rev.*, 2011, **112**, 1196.
- 24 J.-R. Li, J. Sculley and H.-C. Zhou, *Chem. Rev.*, 2011, **112**, 869.
- 25 N. R. Champness, *Dalton Trans.*, 2011, **40**, 10311.
- 26 K. S. Suslick, P. Bhyrappa, J. H. Chou, M. E. Kosal, S. Nakagaki, D. W. Smithery and S. R. Wilson, *Acc. Chem. Res.*, 2005, **38**, 283.
- 27 I. Beletskaya, V. S. Tyurin, A. Y. Tsvadze, R. Guillard and C. Stern, *Chem. Rev.*, 2009, **109**, 1659.
- 28 V. Bulach and M. W. Hosseini, Porphyrin-based tectons in molecular tectonics, in *Handbook of Porphyrin Science*, 2011, vol. 13, p. 299.
- 29 G. M. Sheldrick, *Program for Crystal Structure Solution*, University of Göttingen, Göttingen, Germany, 1997.
- 30 Z. Fang and B. Liu, *Tetrahedron Lett.*, 2008, **49**, 2311.
- 31 L. Yu, K. Muthukumar, I. V. Sazanovich, C. Kirmaier, E. Hindin, J. R. Diers, P. D. Boyle, D. F. Bocian, D. Holten and J. S. Lindsey, *Inorg. Chem.*, 2003, **42**, 6629.
- 32 L. Yu and J. S. Lindsey, *J. Org. Chem.*, 2001, **66**, 7402.
- 33 (a) B. F. Abrahams, B. F. Hoskins and R. Robson, *J. Am. Chem. Soc.*, 1991, **113**, 3606; (b) B. F. Hoskins, D. M. Michail and R. Robson, *Nature*, 1994, **369**, 727.
- 34 C. V. K. Sharma, G. A. Broker, J. G. Huddleston, J. W. Baldwin, R. M. Metzger and R. D. Rogers, *J. Am. Chem. Soc.*, 1999, **121**, 1137.
- 35 K.-J. Lin, *Angew. Chem.*, 1999, **38**, 2730.
- 36 (a) I. Goldberg, *Chem. Commun.*, 2005, 1243; (b) I. Goldberg, *Chem.–Eur. J.*, 2000, **21**, 3863; (c) H. Krupitsky, Z. Stein, I. Goldberg and C. E. Strouse, *J. Inclusion Phenom. Mol. Recognit. Chem.*, 1994, **18**, 177; (d) S. Lipsman, S. Muniappan and I. Goldberg, *Cryst. Growth Des.*, 2008, **8**, 1682.
- 37 L. Carlucci, G. Ciani, D. M. Proserpio and F. Porta, *CrystEngComm*, 2005, **7**, 78.
- 38 B. J. Burnett, P. M. Barron and W. Choe, *CrystEngComm*, 2012, **14**, 3839.
- 39 C. Zou and C.-D. Wu, *Dalton Trans.*, 2012, **41**, 3879.
- 40 (a) B. Zimmer, V. Bulach, M. W. Hosseini, A. De Cian and N. Kyritsakas, *Eur. J. Inorg. Chem.*, 2002, 3079; (b) B. Zimmer, M. Hutin, V. Bulach, M. W. Hosseini, A. De Cian and N. Kyritsakas, *New J. Chem.*, 2002, **26**, 1532; (c) E. Deiters, V. Bulach and M. W. Hosseini, *Chem. Commun.*, 2005, 3906; (d) E. Deiters, V. Bulach and M. W. Hosseini, *New J. Chem.*, 2006, **30**, 1289; (e) E. Deiters, V. Bulach, N. Kyritsakas and M. W. Hosseini, *New J. Chem.*, 2005, **29**, 1508; (f) E. Deiters, V. Bulach and M. W. Hosseini, *New J. Chem.*, 2008, **32**, 99; (g) E. Deiters, V. Bulach and M. W. Hosseini, *Dalton Trans.*, 2007, 4126; (h) E. Kuhn, V. Bulach and M. W. Hosseini, *Chem. Commun.*, 2008, 5104.
- 41 (a) A. Jouaiti and M. W. Hosseini, *Helv. Chim. Acta*, 2009, **92**, 2497; (b) A. Jouaiti, V. Jullien, M. W. Hosseini, J.-M. Planeix and A. De Cian, *Chem. Commun.*, 2001, 1114.
- 42 (a) K. D. Benkstein, C. L. Stern, K. E. Splan, R. C. Johnson, K. A. Walters, F. W. M. Vanheltmont and J. T. Hupp, *Eur. J. Inorg. Chem.*, 2002, 2818; (b) W. H. Otto, M. H. Keefe, K. E. Splan, J. T. Hupp and C. K. Larive, *Inorg. Chem.*, 2002, **41**, 6172.
- 43 S. Tanaka, M. Shirakawa, K. Kaneko, M. Takeuchi and S. Shinkai, *Langmuir*, 2005, **21**, 2163.
- 44 A. Jouaiti, M. W. Hosseini and A. De Cian, *Chem. Commun.*, 2000, 1863.
- 45 A. Jouaiti, M. W. Hosseini and N. Kyritsakas, *Chem. Commun.*, 2002, 1898.
- 46 (a) O. R. Evans and W. Lin, *Acc. Chem. Res.*, 2002, **35**, 511; (b) C. Wang, T. Zhang and W. Lin, *Chem. Rev.*, 2012, **112**, 1084.
- 47 S. M. Le Cours, S. Di Magno and M. J. Therien, *J. Am. Chem. Soc.*, 1996, **118**, 11854.
- 48 R. W. Wagner, T. E. Johnson, F. Li and J. S. Lindsey, *J. Org. Chem.*, 1995, **60**, 5266.
- 49 T. Hayashi, T. Miyahara, N. Koide, Y. Kato, H. Masuda and H. Ogoshi, *J. Am. Chem. Soc.*, 1997, **119**, 7281.
- 50 G. Pognon, J. A. Wytko and J. Weiss, *Org. Lett.*, 2007, **9**, 785.